Assessment of state-of-the-art models for predicting the remobilisation of radionuclides following the flooding of heavily contaminated areas: the case of Pripyat River floodplain

Luigi Monte [a,*], Raul Periañez [b], Sergey Kivva [c], Gennady Laptev [d], Giacomo Angeli [a], Haydn Barros [b], Mark Zheleznyak [c]

[a] *ENEA CR Casaccia, via P. Anguillarese, 301 cp 2400, 00100 Rome, Italy*
[b] *Departamento Fisica Aplicada, University of Sevilla, Spain*
[c] *Institute of Mathematical Machines and System Problems, Ukraine*
[d] *Ukrainian Institute for Hydrometeorology, Ukraine*

Abstract

The performances of models are assessed to predict the wash-off of radionuclides from contaminated flooded areas. This process should be accounted for in the proper management of the aftermath of a nuclear accident. The contamination of the Pripyat River water following the inundation of a floodplain heavily contaminated by ^{90}Sr and ^{137}Cs of Chernobyl origin is used as the basis for modelling. The available experimental evidence demonstrated that remobilisation of radiostrontium is an important process implying a significant secondary radioactive load of water flowing over the contaminated floodplain. On the contrary, there is no empirical evidence of a similar behaviour for radiocaesium. In general, state-of-the-art models properly predicted the remobilisation of strontium, whereas they significantly overestimated radiocaesium concentrations in water. The necessary model improvements for a more accurate prediction of radiocaesium contamination levels include a reassessment of the values of the model parameters controlling the remobilisation process.

Keywords: Modelling; Radionuclides; Contaminated floodplain; Remobilisation

* Corresponding author. Tel.: +39 06 30484645; fax: +39 06 30486716.
E-mail address: monte@casaccia.enea.it (L. Monte).

1. Introduction

A variety of projects were launched, in recent decades, to validate models for predicting the behaviour of radioactive substances in the environment (BIOMOVS, 1990; BIOMOVS II, 1996; IAEA, 2000; BIOMASS, 2003). These projects took advantage of the great deal of experimental data gathered to assess the contamination levels of ecosystem components and of the human food chain following the accidental introduction of radionuclides into the environment.

Recently, the International Atomic Energy Agency (IAEA) has initiated the project EMRAS (Environmental Modelling for Radiation Safety) that continues some of the activities of previous international programmes of radioecological modelling (http://www-ns.iaea.org/projects/emras/). One of the working groups involved in the project focused on the validation of models for radionuclide transport in the aquatic system.

A number of validation exercises were performed in this field (BIOMOVS, 1990; IAEA, 2000), and model review and assessment studies demonstrated that the results achieved during past decades by researchers have produced some consolidated results that are, generally, widely accepted by most modellers (Monte et al., 2003, 2004, 2005a,b). Nevertheless, there are some particular features of models that have not been sufficiently analysed and tested in the past. Among these, the simulation of the secondary radioactive load of river waters from heavily contaminated flooded areas is of particular importance.

This work aims at assessing the performances of three state-of-the-art models for predicting the secondary contamination of the Pripyat River water following the inundation of the contaminated Chernobyl floodplain. The modelling exercise was performed for ^{137}Cs and ^{90}Sr, two radionuclides of significant environmental importance. It supplies useful information concerning the mobility of these radionuclides in the aquatic environment.

2. Description of the environmental scenario

The Pripyat River floodplain is an embanked area, 12-km long and 4-km wide, adjacent to the Chernobyl nuclear power plant (Fig. 1). The Pripyat River enters the study area near the exclusion zone boundary (the ''input section'') and flows out near the Yanov Bridge (the ''output section''). The floodplain received a heavy impact of radioactive contamination after the Chernobyl accident in 1986 (Voitsekhovich et al., 1991).

In January 1991, an ''ice jam'' formed in the Pripyat River channel between the Yanov Bridge and the town of Chernobyl. The water level in the Pripyat River upstream of the jam increased abruptly. Consequently, a significant part of the Pripyat River floodplain near the nuclear power plant was flooded for the first time since the accident. This caused washout of radionuclides into the river and resulted in a significant increase of ^{90}Sr concentration in the whole Dnieper River cascade. The water level then decreased to normal values. The construction of a protective sand dike on the left bank of the floodplain to prevent radionuclide wash-off to the River Pripyat was proposed (Zheleznyak and Voitsekhovich, 1991; Zheleznyak et al., 1992, 1997) and constructed during 1991−1992.

An extremely high spring flood occurred in 1999 while the construction of an additional protective dam on the right bank of Pripyat River was in the initial phase. The maximum water discharges in the river were as high as 3000 $m^3 s^{-1}$ and were the highest reported in the river since the historically high flood of 1979 (4500 $m^3 s^{-1}$). Because the construction of the dam on

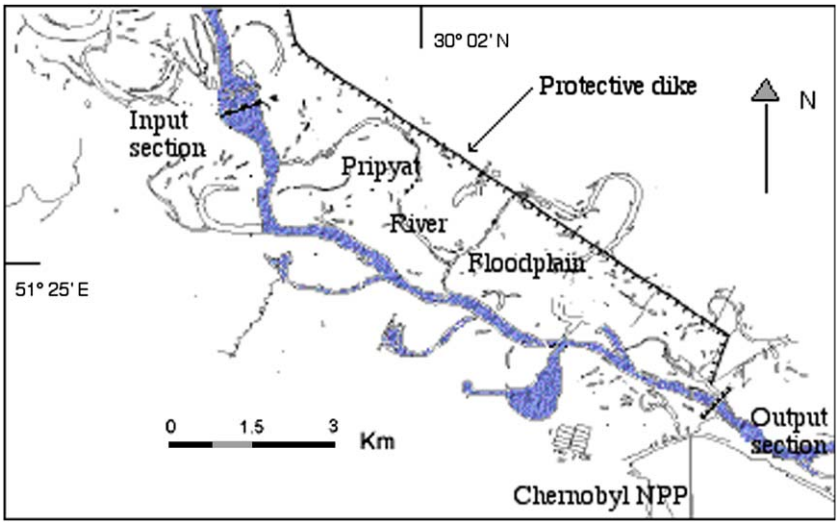

Fig. 1. The Pripyat River floodplain.

the right bank was not completed, part of the right bank floodplain was flooded for almost two weeks, mainly due to dam overflow. The dam did not prevent wash-off from the floodplain, but only lengthened the formation of floodplain flows and reduced a possibly higher peak in the river contamination, which could have occurred with more rapid flow of water from the floodplain. Completion of the dikes on the left and right banks has proven effective for reducing ^{90}Sr loads (Smith et al., 2001).

The following data and information were supplied to the modellers (Voitsekhovich et al., 2004):

- the topography of the floodplain including data on protective dikes configuration in different periods;
- the deposition density of ^{137}Cs and ^{90}Sr on the floodplain;
- physico-chemical forms of ^{137}Cs and ^{90}Sr in floodplain soil;
- chemical characteristics of the Pripyat River water;
- granulometric characteristics of suspended sediment;
- hydrological and meteorological data (daily values of water levels, water discharge at the input section of the floodplain, etc.);
- concentrations of ^{137}Cs (the dissolved and particulate phases) and ^{90}Sr (the dissolved phase) in the ''input cross section'' of Pripyat River (generally, weekly samplings).

All the data and information supplied were gathered and selected by independent experts involved in the assessment of the aftermath of the Chernobyl accident in Ukraine.

3. Main characteristics of the models

The models used in the present exercise were developed by the University of Sevilla (Spain), the ENEA (Italy) and the IMMSP (Ukraine) and are described in Appendix A. They are based

on methodologies and approaches that are commonly used by state-of-the-art models aimed at assessing the behaviour of radionuclides in the freshwater environment.

Each model is composed of a hydrological module aimed at evaluating the water fluxes and, consequently, the dynamic of the floodplain inundation and, a radionuclide migration model. The present work does not focus on the assessment of the features of the hydrological modules. Our aim is to evaluate and compare the radionuclide migration sub-models. The University of Sevilla model was implemented in two different versions (-3C and -4C) as described in Appendix A.

The analysis of the mathematical features of the three models demonstrates that they show similar basic structures. Indeed, their equations can be written in the following common form:

$$\begin{aligned}
\frac{\partial hC}{\partial t} &= -\left(k_{\mathrm{wf}} + k_{\mathrm{ws}} + \lambda\right)hC + k_{\mathrm{fw}}D_{\mathrm{f}} + k_{\mathrm{sw}}D_{\mathrm{s}} - \mathrm{dil} + [(\mathrm{adv} + \mathrm{dif})hC] \\
\frac{\partial D_{\mathrm{f}}}{\partial t} &= k_{\mathrm{wf}}hC - \left(k_{\mathrm{fw}} + k_{\mathrm{fs}} + \lambda\right)D_{\mathrm{f}} + k_{\mathrm{sf}}D_{\mathrm{s}} \\
\frac{\partial D_{\mathrm{s}}}{\partial t} &= k_{\mathrm{ws}}hC + k_{\mathrm{fs}}D_{\mathrm{f}} - \left(k_{\mathrm{sf}} + k_{\mathrm{sw}} + k_{\mathrm{s}} + \lambda\right)D_{\mathrm{s}}
\end{aligned} \tag{1}$$

where adv and dif represent, respectively, the advection and diffusion operators, dil is the dilution operator accounting for the variation with time of the water volume, C is the concentration of dissolved radionuclide in water (Bq m^{-3}), D_{f} and D_{s} are, respectively, the radionuclide per square metre (Bq m^{-2}) in the ''fast'' and ''slow'' interactive fractions of particulate radionuclide and h is the depth of the water body. The term hC is the dissolved radionuclide per square metre in the water column (Bq m^{-2}). λ is the radioactive decay constant (s^{-1}). The mathematical form of Eq. (1) makes quite apparent the meanings of the terms hC, D_{f} and D_{s} (radionuclide amount per square metre in each environmental component) and of the products of these terms by the rates k_{ij} (s^{-1}) (the fluxes of radionuclide per square metre exchanged among the system components). A list of symbols in Eq. (1) is reported in Table 1. The comprehensive structure of the sub-model controlling the radionuclide interaction with sediment is shown in Fig. 2. It should be noted that: (a) in University of Sevilla-3C model D_{f} and D_{s} are defined as the ''reversible'' and the ''slow reversible'' radionuclide fractions in sediment; (b) in ENEA model, D_{f} is the radionuclide in suspended matter and in a very thin layer of soil strongly interacting with radionuclide in water (it is assumed that the radionuclide concentration in such a layer is equal to the concentration in suspended matter), D_{s} is the radionuclide deposit in the contaminated soil; and (c) in model COASTOX, developed by the IMMSP, D_{f} and D_{s} correspond, respectively, to the radionuclide in suspended matter and in the upper soil layer of the floodplain.

The University of Sevilla-4C model considers four compartments that correspond to radionuclide in water (dissolved phase), radionuclide in suspended matter and radionuclide concentrations in floodplain soil (fast and slow exchangeable forms).

The models COASTOX and University of Sevilla-3C and -4C implemented the advection and diffusion terms by well-known partial differential equations.

Model ENEA simulated the diffusion and the advection processes by subdividing the water body into sectors covering the river and the floodplain. The radionuclide fluxes between two contiguous sectors were calculated accounting for the water fluxes exchanged between these sectors.

Table 1
List of symbols in Eq. (1)

Symbol	Description	Dimension
C	Radionuclide concentration in water (dissolved form)	Bq m^{-3}
D_f	Radionuclide (particulate phase) per square metre (fast component)	Bq m^{-2}
D_s	Radionuclide (particulate phase) per square metre (slow component)	Bq m^{-2}
k_{wf}	Radionuclide migration rate from water (dissolved form) to particulate phase (first exchange process)	s^{-1}
k_{ws}	Radionuclide migration rate from water (dissolved form) to particulate phase (second exchange process)	s^{-1}
k_{fw}	Radionuclide migration rate to water (dissolved form) from particulate phase (first exchange process)	s^{-1}
k_{sw}	Radionuclide migration rate to water (dissolved form) from particulate phase (second exchange process)	s^{-1}
k_{fs}	Radionuclide migration rate from the first to the second component of radionuclide particulate phase	s^{-1}
k_{sf}	Radionuclide migration rate from the second to the first component of radionuclide particulate phase	s^{-1}
k_s	Radionuclide fixation rate (irreversible process)	s^{-1}
λ	Radioactive decay constant	s^{-1}
h	Depth of the water column	m

The matrix of the coefficients of Eq. (1), when the dilution, the advection and the diffusion terms are not accounted for, is

$$\begin{vmatrix} -(k_{wf}+k_{ws}+\lambda) & k_{fw} & k_{sw} \\ k_{wf} & -(k_{fw}+k_{fs}+\lambda) & k_{sf} \\ k_{ws} & k_{fs} & -(k_{sf}+k_{sw}+k_s+\lambda) \end{vmatrix} \tag{2}$$

The above coefficients control the behaviour of radionuclides in the sub-system water−soil.

The matrices of the model coefficients, once the models are transformed into form (1), are as follows:

Model University of Sevilla-3C:

$$\begin{vmatrix} -\left(\frac{3L\Psi\chi_1}{Rh}(1-\Phi)+\lambda\right) & \frac{3\chi_1}{k_d\rho_b R}\Psi & 0 \\ \frac{3L\Psi\chi_1}{Rh}(1-\Phi) & -\left(\frac{3\chi_1}{k_d\rho_b R}\Psi+k_3+\lambda\right) & k_4 \\ 0 & k_3 & -(k_4+\lambda) \end{vmatrix} \tag{3}$$

Model ENEA:

$$\begin{vmatrix} -\left(k_{12}+\frac{v_{ws}}{h}+\lambda\right) & \frac{k_{12}}{f_{p/d}+\Delta h/h} & 0 \\ k_{12} & -\left(\frac{k_{12}}{f_{p/d}+\Delta h/h}+\lambda\right) & K_{sw} \\ \frac{v_{ws}}{h} & 0 & -(K_{sw}+K_{ds}+\lambda) \end{vmatrix} \tag{4}$$

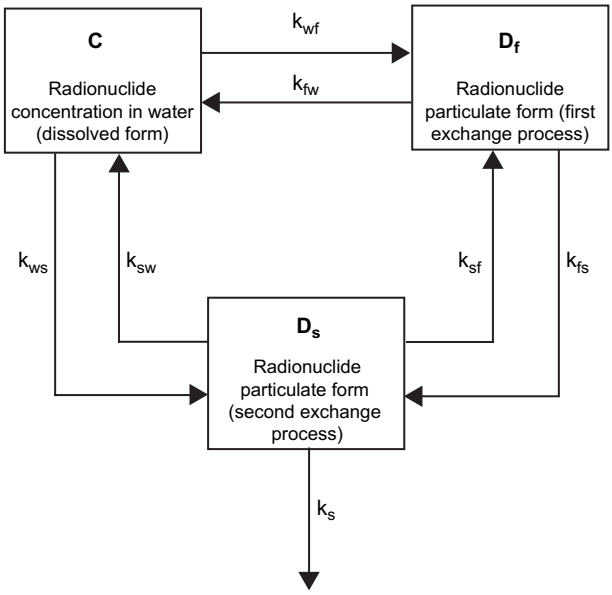

Fig. 2. Comprehensive structure of sub-models for predicting the behaviour of radionuclide in the water-sediment system. Model ENEA hypothesises that compartments C and D_f are at equilibrium.

Model COASTOX (exchangeable phase):

$$\begin{vmatrix} -\left(a_s S_m \frac{k_d^s}{\rho} + \frac{(1-\Phi) L a_b k_d^b \frac{\rho_b}{\rho}}{h} + \lambda\right) & a_s & a_b \\ a_s S_m \frac{k_d^s}{\rho} & -\left(a_s + \frac{q_s}{h S_m} + \lambda\right) & \frac{q_b}{(1-\Phi) L \rho_b} \\ \frac{(1-\Phi) L a_b k_d^b \frac{\rho_b}{\rho}}{h} & \frac{q_s}{h S_m} & -\left(a_b + \frac{q_b}{(1-\Phi) L \rho_b} + \lambda\right) \end{vmatrix} \quad (5)$$

Model COASTOX simulated the sedimentation and resuspension of radionuclide in fuel particles and in non-exchangeable phase by equations that are structurally similar to the ones controlling the corresponding processes for the exchangeable phase although are independent of these last (uncoupled equations).

The previous matrices allow comparison of the features of the models in relation to the process of radionuclide interaction with inundated soil.

A list of symbols in matrices (3)−(5) is reported in Table 2. As previously observed, the assessed models (except University of Sevilla-4C which is composed of four compartments) show a common comprehensive mathematical structure. Therefore, for suitable choices of the values of the model parameters, similar approximate features of the model results can be expected in relation to the processes of radionuclide interaction with soil and particulate matter, although the model solutions are different from a rigorous mathematical point of view.

Table 2
List of symbols in matrices in Eqs. (3)–(5)

Symbol	Description	Model	Dimension
a_s	Radionuclide exchange rate water-suspended sediment	COASTOX	s^{-1}
a_b	Radionuclide exchange rate water-upper soil layer	COASTOX	s^{-1}
$f_{p/d}$	Ratio radionuclide in particulate form/radionuclide in dissolved form (in the water column)	ENEA	Dimensionless
k_{12}	Rate of transformation of radionuclide from water (dissolved form) to particulate phase (first exchange process)	ENEA	s^{-1}
K_{sw}	Radionuclide migration rate from bottom sediments to water	ENEA	s^{-1}
K_{ds}	Radionuclide migration rate from bottom sediments to buried sediments (corresponding to k_s)	ENEA	s^{-1}
k_d^s	Dimensionless radionuclide partition coefficient ''suspended sediment/water'' (radionuclide concentration in suspended sediment in $Bq\,kg^{-1}$ divided by dissolved radionuclide concentration in water in $Bq\,kg^{-1}$)	COASTOX	Dimensionless
k_d^b	Dimensionless radionuclide partition coefficient ''upper soil layer/water'' (radionuclide concentration in upper soil layer in $Bq\,kg^{-1}$ divided by dissolved radionuclide concentration in water in $Bq\,kg^{-1}$)	COASTOX	Dimensionless
k_d	Radionuclide partition coefficient	Sevilla U.	$m^3\,kg^{-1}$
k_3, k_4	Rates of radionuclide exchange between reversible and slowly reversible fractions of sediments	Sevilla U.	s^{-1}
L	Thickness of active soil layer	COASTOX Sevilla U.	m
q_s	Sedimentation rate	COASTOX	$kg\,m^{-2}\,s^{-1}$
q_b	Resuspension rate	COASTOX	$kg\,m^{-2}\,s^{-1}$
R	Average radius of sediment particles	Sevilla U.	m
S_m	Concentration of suspended sediment in water	COASTOX Sevilla U.	$kg\,m^{-3}$
v_{ws}	Radionuclide migration velocity from water to bottom sediments	ENEA	$m\,s^{-1}$
Δh	Incremental depth (see description of model ENEA in Appendix A)	ENEA	m
ρ	Density of water	COASTOX	$kg\,m^{-3}$
ρ_b	Density of soil matrix/particle density	COASTOX, Sevilla U.	$kg\,m^{-3}$
Φ	Porosity of soil	COASTOX Sevilla U.	Dimensionless
χ_1	Exchange velocity (see description of University of Sevilla model in Appendix A)	Sevilla U.	$m\,s^{-1}$
Ψ	Correction factor (see description of University of Sevilla model in Appendix A)	Sevilla U.	Dimensionless

In spite of that, the models are based on conceptual approaches that are significantly dissimilar. Model ENEA makes use of aggregated parameters, v_{ws}, k_{sw} and k_{ds}, that were estimated by previous applications of the model to a variety of freshwater systems contaminated by the examined radionuclides (''aggregated model''). The University of Sevilla and COASTOX models determine the values of the transfer parameters by formulae that relate these values to some physical, chemical and geological characteristics of the environmental compartments and of radionuclides (''reductionistic models''). As found in previous assessments of state-of-the-art models for predicting the behaviour of radionuclides in lakes and rivers (Monte et al., 2003, 2005a), most models belong to one of the above categories. The advantages and the disadvantages of these approaches were deeply debated in the scientific literature (Jørgensen, 1983;

Jørgensen and Mejer, 1979; Håkanson and Monte, 2003). Some modellers deem the use of aggregated parameters in models as a source of uncertainty unless site-specific values are available. Nevertheless, it should be noted that, frequently, the parameters in ''reductionistic'' models are calculated from generic quantities, such as a_b (radionuclide exchange rate ''water-upper soil layer'' in COASTOX model) and χ_1 (radionuclide exchange ''velocity'' between dissolved and particulate forms in University of Sevilla model), that significantly influence the uncertainty of the model depending on the assumptions substantiating the selection of the relevant values.

4. Results

The assessment of the model performances compared the model output with empirical concentrations of radionuclides in water collected at the ''output'' cross section of the floodplain (Fig. 1). The empirical data cover periods of time from, approximately, one month before the flooding event to one month after the event. The sampling frequency was of the order of the week.

The first phase of the exercise was a ''blind test'' (the empirical data of water contamination at the ''output'' section of the floodplain were not disclosed to modellers) of the University of Sevilla-3C and ENEA models applied to the 1991 flooding event. COASTOX model was applied, since the early nineties, for this floodplain modelling as a part of the studies for justification of water protection measures (Zheleznyak et al., 1992, 1997). Consequently, COASTOX did not participate in this phase of the exercise as the developers of this model had access to the empirical data.

Figs. 3 and 4 show the model results obtained for the flooding event in 1991. As seen from the figures, both models predicted the increase of ^{90}Sr concentration in water, following the inundation of the floodplain. It should be noted that the time behaviour of the contamination is influenced by the flooding dynamics that, in view of the lack of sufficient information, was not properly accounted for at this stage of the exercise; this gives reason of the differences in the radiocontamination decline with time of the model output and the empirical data. On the contrary (Fig. 4), the models significantly overestimated the concentration of ^{137}Cs in water.

Following the first phase of the exercise based on the above described blind test, the output data were disclosed and modellers were asked to carry out new model applications (exercise phase-2).

The new results of the models were obtained by using parameter values that better reflected the low remobilisation of ^{137}Cs from soil. The application of the University of Sevilla model was done by considering a fourth compartment to simulate more accurately the interaction of radionuclide with the suspended matter. The calibrated models were also applied to the flooding event occurred in 1999. The results of these further applications are shown in Figs. 5 and 6.

5. Discussion

It should be noted that the most important factor influencing the contamination of water in the floodplain is the remobilisation of radionuclide from the heavily contaminated soil. The blind test exercise clearly showed the propensity of modellers to hypothesise a significant remobilisation of contaminants from the polluted floodplain. The comparison of the model results

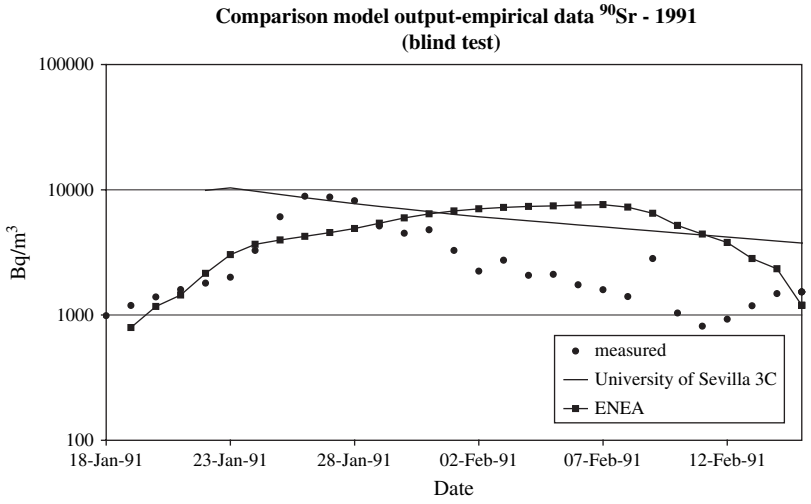

Fig. 3. Comparison of model predictions with empirical data of ^{90}Sr concentration in Pripyat River (‘‘output section’’). Results obtained from a ‘‘blind test’’ of model validation. The inundation caused a significant increase of radionuclide concentration in the river water as predicted by the models. It should be noted that no sufficient information and data were used by the modellers for an accurate simulation of the dynamics of the floodplain inundation. Consequently, the model predictions did not fit accurately the decline of radionuclide contamination levels that reflects such a complicated dynamics. COASTOX did not participate in this phase of the exercise as the developers of this model had access to the empirical data (see the text).

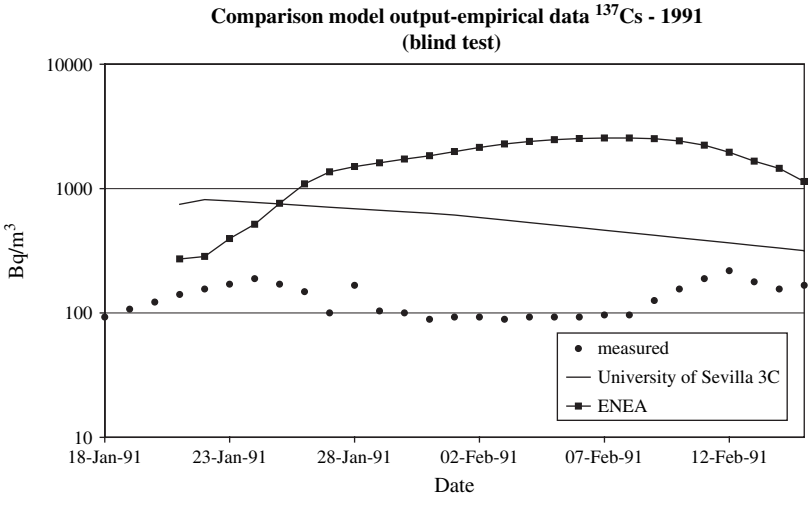

Fig. 4. Comparison of model predictions with empirical data of ^{137}Cs concentration in Pripyat River water (‘‘output section’’). Results obtained from a ‘‘blind test’’ of model validation. The inundation did not cause the significant increase of radionuclide concentration in the river water predicted by the models. COASTOX did not participate in this phase of the exercise as the developers of this model had access to the empirical data (see the text).

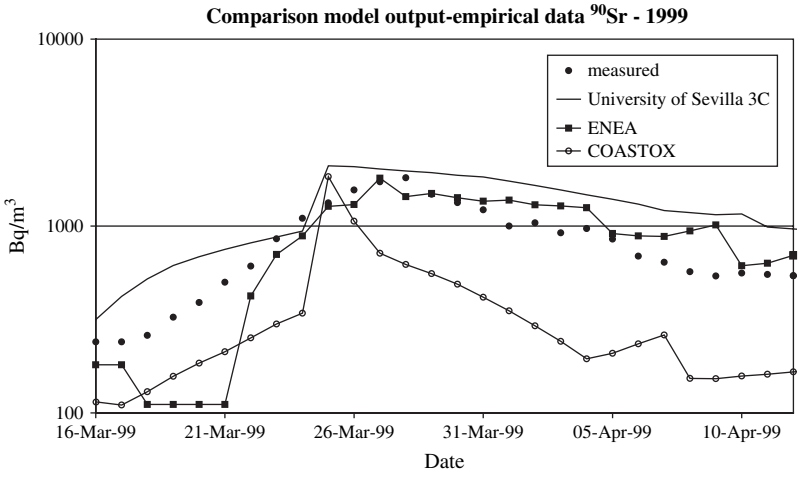

Fig. 5. Comparison of model output and experimental concentrations of ^{90}Sr in the ''output section'' of the floodplain in 1999.

with the empirical data clearly demonstrated that such a hypothesis is valid for ^{90}Sr but should be used with caution for ^{137}Cs.

A great deal of studies demonstrated that ^{137}Cs shows a lower mobility than ^{90}Sr (Frissel and Pennders, 1983; Livens and Rimmer, 1988; McHenry and Ritchie, 1977; Ritchie and McHenry, 1990). These results were generally accounted for by modellers as demonstrated, for instance, by the ratios v_{ws}/k_{sw} and the values of k_{ds} for caesium and strontium used by the ENEA model for the blind test application (Table 3). The higher value of the ratio v_{ws}/k_{sw} for ^{137}Cs indicates a more intense migration of this radionuclide from water to sediment. Moreover the high value of k_{ds} denotes a more efficient burial of radionuclide and a consequent significant decrease of its

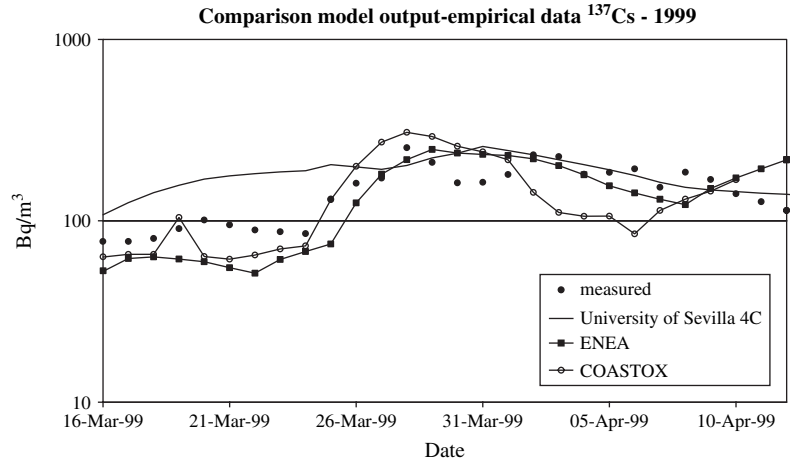

Fig. 6. Comparison of model output and experimental concentrations of ^{137}Cs in the ''output section'' of the floodplain in 1999.

Table 3
Values of the parameters in the "water-sediment" radionuclide migration sub-model of model ENEA (Monte, 2001; Monte et al., 2003)

Parameter	Description	Units	^{90}Sr (blind test)	^{137}Cs (blind test)	^{137}Cs (calibrated)
v_{ws}	Radionuclide migration velocity to sediment	m s^{-1}	1.0×10^{-7}	1.6×10^{-6}	2.8×10^{-5}
k_{sw}	Radionuclide resuspension rate from sediment to water	s^{-1}	5.6×10^{-9}	1.5×10^{-8}	5.0×10^{-9}
k_{ds}	Radionuclide migration rate to deep sediment	s^{-1}	8.8×10^{-10}	1.2×10^{-8}	1.2×10^{-9}
$f_{p/d}$	Radionuclide in particulate form/radionuclide in dissolved form	Dimensionless	≈ 0	≈ 1	≈ 1
Δh	Incremental depth	m	0	6	18

remobilisation rate. In spite of these values, this exercise demonstrated that the remobilisation of caesium was yet overestimated by state-of-the-art models. Table 3 shows the calibrated values of the migration parameters used for a more accurate simulation of the behaviour of radiocaesium.

From the coefficient matrices, it is possible to calculate and compare the values of the migration velocity to sediment of ^{137}Cs used by the different models. The following formula

$$(1 - \Phi) L a_b k_d^b \frac{\rho_b}{\rho} \tag{6}$$

was used by COASTOX. Supposing $\Phi = 0.5$, $a_b = 5.7 \times 10^{-7}$ s^{-1}, $k_d^b = 4500$, $\rho = 1000$ kg m^{-3}, $\rho_b = 2600$ kg m^{-3} and $L = 0.05$ m we get a value of 1.7×10^{-4} m s^{-1}.

The migration velocity to sediment used by the University of Sevilla-4C model is

$$\frac{3L\Psi}{R}(\chi_{11} + \chi_{12})(1 - \Phi) \tag{7}$$

where χ_{11} and χ_{12} are the exchange velocity for the fast and slow interaction of dissolved radionuclide with suspended matter. Supposing (Periáñez, 2004) that $\chi_{12} \ll \chi_{11} = 1.4 \times 10^{-5}$ m s^{-1}, $R = 10$ μm, $\Psi = 5 \times 10^{-2}$, we obtain from formula (7) a value of the order of 10^{-3} m s^{-1}.

The value used by the calibrated version of the ENEA model for application to the 1999 event was 2.8×10^{-5} m s^{-1}. It should be noticed that, as seen from matrices (4) and (5), the flux of radionuclide from water to soil calculated by model COASTOX is $(1 - \Phi) L a_b k_d^b (\rho_b/\rho) C + (q_s/h S_m) D_f$ whereas model ENEA determines such a flux as $v_{ws} C$ by using a generic value of the radionuclide deposition velocity. This last parameter aggregates the processes of radionuclide direct interaction with soil particles and the radionuclide sedimentation.

At any rate, beyond the differences among the three models, the order of magnitude of the values of the migration velocity to sediment used by the ENEA and University of Sevilla-3C models for the blind test was significantly lower than the calibrated ones. The University of Sevilla-3C model used $\chi_1 = 2.0 \times 10^{-7}$ m s^{-1} for ^{137}Cs that is two orders of magnitude lower than $\chi_{11} = 1.4 \times 10^{-5}$ m s^{-1} in the Sevilla-4C model.

It is worthwhile to note that different sets of values of the migration parameters can be used to obtain model results matching with the empirical data, provided that high overall

radionuclide fluxes from water to sediment are simulated. High overall fluxes can be obtained in several ways by selecting different sets of values of the rate of irreversible fixation of radionuclide on soil (k_s), of the remobilisation rates (k_{sw}, k_{fw}) and of the rates of radionuclide migration from water to soil (k_{ws}, k_{wf}). In view of the uncertainties of the empirical data (radionuclide concentrations in water and the spatial distribution of the radionuclide deposition on the floodplain), the lack of detailed information concerning the flooding dynamics, the variability in space of the floodplain characteristics (for instance, the nature of soil), the sensitivity of the models, etc., it is difficult to determine an unequivocal ''calibrated'' set of parameter values. As an example, Fig. 7 shows the results of four simulations obtained by using different values of v_{ws}, K_{sw} and K_{ds} in model ENEA. As the figure demonstrates, even with the wide range of parameter values, the model results do not show appreciable differences that would allow one to select unequivocally the optimal values of these parameters.

As stated in the previous paragraph, the models calibrated to the flooding event in 1991 were subsequently applied to the flooding occurred in 1999. These applications (Figs. 5 and 6) clearly demonstrated that the models performed appropriately for an event different from the calibration conditions. This result supports the suggested model improvements.

The time behaviour of radionuclide concentration in water is very sensitive to the dynamics of flooding. Indeed, the concentration of radionuclides in water depends on the time of inundation of areas showing different contamination levels and on the proportion of water flowing on more or less contaminated areas. Therefore, the results of the ''phase-2'' exercise of University of Sevilla and ENEA models were obtained following a ''calibration'' of the hydrological modules of the models to assure that the predicted time behaviour of radionuclide in water was compatible with the empirical data. On the contrary, the results of model COASTOX were obtained, for the present exercise, without special tuning of the hydrological module. It should be kept in mind that the present work, as previously stated, is not aimed at evaluating the hydrological modules of the above models and that the complexity of the inundation dynamics and

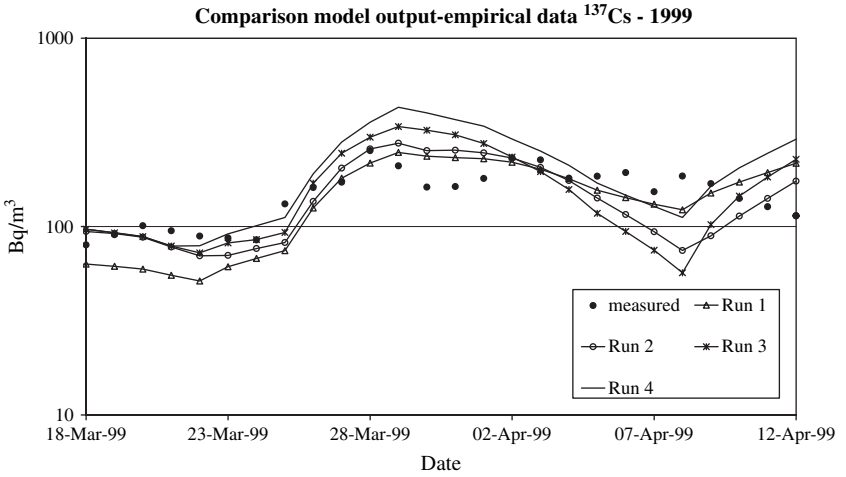

Fig. 7. Comparison of the results of four simulations from model ENEA for different values of the model parameters: Run 1, $v_{ws} = 2.8 \times 10^{-5}$ m s^{-1}, $k_{sw} = 5.0 \times 10^{-9}$ s^{-1}, $k_{ds} = 1.2 \times 10^{-9}$ s^{-1}, $\Delta h = 18$ m; Run 2, $v_{ws} = 1.6 \times 10^{-6}$ m s^{-1}, $k_{sw} = 0$ s^{-1}, $k_{ds} = 0$ s^{-1}, $\Delta h = 24$ m; Run 3, $v_{ws} = 1.6 \times 10^{-6}$ m s^{-1}, $k_{sw} = 0$ s^{-1}, $k_{ds} = 0$ s^{-1}, $\Delta h = 6$ m; Run 4, $v_{ws} = 1.6 \times 10^{-5}$ m s^{-1}, $k_{sw} = 1.0 \times 10^{-9}$ s^{-1}, $k_{ds} = 0$ s^{-1}, $\Delta h = 6$ m.

the large amount of data necessary to predict its time behaviour prevented from testing the predictive features of these hydrological modules.

6. Conclusions

Radionuclide remobilisation is considered one of the most important factors controlling the amount of radionuclide in waters inundating highly contaminated areas. One of the aims of this exercise was to test the performances of state-of-the-art models for predicting such an important process. The experimental evidence from the inundation events of the Chernobyl floodplain demonstrated that remobilisation of radiostrontium from contaminated soils is an important process implying a significant secondary radioactive load of water flowing over contaminated floodplains. On the contrary, there is no empirical evidence of a similar behaviour for radiocaesium.

The remobilisation of strontium was properly predicted, whereas it was significantly overestimated for caesium as demonstrated by the blind tests.

The results should be accounted for the improvement of models aimed at supporting the management of the aftermath of nuclear accidents. It was also demonstrated that the predictions of the hydrological processes should be done with reasonable accuracy in order to reduce the uncertainty of radionuclide transport forecasting.

Acknowledgements

The Floodplain scenario was developed by Oleg Voitsekhovich and Gennady Laptev of the Ukrainian Hydrometeorological Institute, Kiev, Ukraine and by Alexei Konoplev and Anatoly Bulgakov of the Centre for Environmental Chemistry of SPA ''Typhoon'', Obninsk, Russia. The present work was carried out in the frame of project EMRAS (Environmental Modelling for Radiation Safety) organised by IAEA.

Appendix A. Model descriptions

A.1. University of Seville

A 2D, depth-averaged model was used. The model solves the hydrodynamic equations to obtain water circulation. The output from the hydrodynamic model is used to solve the advection/diffusion dispersion equation for radionuclides. Depth-averaged shallow water hydrodynamic equations may be written in the form:

$$\begin{aligned}
&\frac{\partial z}{\partial t}+\frac{\partial}{\partial x}(hu)+\frac{\partial}{\partial y}(hv)=0\\
&\frac{\partial u}{\partial t}+u\frac{\partial u}{\partial x}+v\frac{\partial u}{\partial y}+g\frac{\partial z}{\partial x}-\Omega v+k\frac{u\sqrt{u^2+v^2}}{h}=0\\
&\frac{\partial v}{\partial t}+u\frac{\partial v}{\partial x}+v\frac{\partial v}{\partial y}+g\frac{\partial z}{\partial y}+\Omega u+k\frac{v\sqrt{u^2+v^2}}{h}=0
\end{aligned} \tag{A1}$$

where u and v are the components of the water current along x and y axis, h is depth of the water column and z is the displacement of the water surface: $h = z - d$ (d is topographic height). Ω is

the Coriolis parameter and k is a bed friction coefficient obtained from model calibration. Equations have been solved by finite differences on a grid covering the floodplain area with a resolution $\Delta x = \Delta y = 200$ m. A steady-state approach has been assumed. Thus, the hydrodynamic model has been forced by constant surface elevations along input and output cross sections and calculations are continued until a steady-state for currents and elevations is obtained for the whole model domain. The following condition has been applied to the water current component (ξ) normal to the boundary:

$$\frac{\partial \xi}{\partial \eta} = 0 \tag{A2}$$

where η is the coordinate normal to the boundary.

The calibration of the bed friction coefficient was carried out by trial and error assessment until the computed water discharge through the output section was as close as possible to the measured discharge. Using $k = 0.030$, a discharge equal to 483.4 $m^3 s^{-1}$ is computed, which can be compared with discharges measured during the first flood event.

The exchanges of radionuclides between the liquid and solid phases are described by means of kinetic coefficients. The rate coefficient k_1 governs the transfer from the dissolved to the solid phase and the rate coefficient k_2 governs the inverse process.

The adsorption of radionuclides depends on the available surface of particles per water volume unit:

$$k_1 = \chi_1 \sigma \tag{A3}$$

where χ_1 is a coefficient with the dimensions of a velocity (denoted exchange velocity) and σ is the specific surface (dimension m^{-1}). Assuming spherical particles with an average radius R, we get:

$$\sigma = \frac{3L\Psi}{Rh}(1 - \Phi) \tag{A4}$$

where L is the average mixing depth (the sediment depth at which the water fraction exchanges radionuclides with the sediment), Φ is the sediment porosity and Ψ is a correction factor accounting for the effective surface of sediment particles that is in contact with water since particles can partially overlap one another.

The 3C model considers that exchanges are governed by two consecutive reversible reactions. Surface adsorption is followed by another slower process that may be a slow diffusion of ions into pores and inter-lattice spaces, inner complex formation or a transformation such an oxidation. Thus, sediments/soils are divided into two phases: a reversible and a slowly reversible fraction. The equations that give the time evolution of activity concentrations in the three phases are

$$\begin{aligned}
\frac{\partial C}{\partial t} &= (\mathrm{adv} + \mathrm{dif}) - k_1 C + k_2 \frac{A_r L \rho_s \Psi}{h} - \lambda C \\
\frac{\partial A_r}{\partial t} &= k_1 \frac{Ch}{L\rho_s} - k_2 A_r \Psi - k_3 A_r + k_4 A_{sr} - \lambda A_r \\
\frac{\partial A_{sr}}{\partial t} &= k_3 A_r - k_4 A_{sr} - \lambda A_{sr}
\end{aligned} \tag{A5}$$

where C is the concentration of radionuclide in the dissolved phase (Bq m^{-3}), A_r and A_{sr} are, respectively, radionuclide concentrations in the reversible and slowly reversible fractions of

sediments and the bed (Bq kg^{-1}), ρ_s is sediment bulk density, k_3 and k_4 are the forward and backward rates governing the second reaction and λ is the radioactive decay constant.

Advection and diffusion terms are written in the following form:

$$\begin{aligned} \text{adv} &= -\frac{1}{h}\left(\frac{\partial(Ch)}{\partial x}+\frac{\partial(Ch)}{\partial y}\right) \\ \text{dif} &= \frac{1}{h}\left(\frac{\partial}{\partial x}\left(hK\frac{\partial C}{\partial x}\right)+\frac{\partial}{\partial y}\left(hK\frac{\partial C}{\partial y}\right)\right) \end{aligned} \tag{A6}$$

where K is a diffusion coefficient. This coefficient depends on grid size, following classical relations, and results $K = 0.091\ m^2\ s^{-1}$.

Boundary conditions must also be provided to solve the dispersion equations. In the input section, activity concentrations in water are specified from the measurements. Along the output section, a condition of zero gradient along the normal direction (as in the case of water currents) is used.

The exchange velocity and k_2 are related to the equilibrium distribution coefficient by the following relation:

$$k_d = \frac{\chi_1}{k_2}\frac{3}{\rho_b R} \tag{A7}$$

where k_d is the equilibrium distribution coefficient and ρ_b is density of particles. It has been found that parameter k_2 remains rather constant even for elements with a rather different geochemical behaviour. Thus, we have used the same value as in previous caesium modelling applications: $k_2 = 1.16 \times 10^{-5}\ s^{-1}$. The average particle radius, from provided information, has been fixed as 10 μm and a standard value for particle density is 2600 kg m^{-3}. Thus, from these parameters and a site-specific distribution coefficient it is possible to have a site-specific value for the exchange velocity. The distribution coefficient of ^{137}Cs has been taken, from literature, as 2.0 $m^3\ kg^{-1}$. This implies an exchange velocity equal to $2.00 \times 10^{-7}\ m\ s^{-1}$. The kinetic rates for the second reaction in the 3C model have been taken as follows: $k_3 = 1.20 \times 10^{-7}\ s^{-1}$ and $k_4 = 1.20 \times 10^{-8}\ s^{-1}$. Sediment bulk density has been taken as $\rho_s = 1300\ kg\ m^{-3}$.

Two other parameters have values that must be defined. They are the sediment mixing depth L and the correction factor Ψ. Model results are sensitive to the values chosen for L and Ψ. A choice of these parameters was $\Psi = 0.05$ and $L = 0.05$ m.

The dispersion model has been run for 59 days, in the case of the first event (1991 ice jam). The model provides activity concentration in the dissolved phase in the output section along the 59 days of simulation.

The normalised form of the model is

$$\begin{aligned} \frac{\partial hC}{\partial t} &= (\text{adv}+\text{dif}) - k_1 hC + k_2 \Psi D_f - \lambda C \\ \frac{\partial D_f}{\partial t} &= k_1 hC - k_2 D_f \Psi - k_3 D_f + k_4 D_s - \lambda D_f \\ \frac{\partial D_s}{\partial t} &= k_3 D_f - k_4 D_s - \lambda D_s \end{aligned} \tag{A8}$$

The 4C model includes a further compartment to describe the kinetic process of interaction of radionuclide with suspended matter and bottom sediments:

$$\begin{aligned}
\frac{\partial C}{\partial t} &= (\mathrm{adv}+\mathrm{dif}) - \chi_{11}\frac{3S_\mathrm{m}}{\rho_\mathrm{b}R}C - (\chi_{11}+\chi_{12})\frac{3L\Psi}{Rh}(1-\Phi)C + k_{21}S_\mathrm{m}C_\mathrm{s} \\
&\quad + \frac{L\rho_\mathrm{b}\Psi}{h}(1-\Phi)(k_{21}C_\mathrm{sed1} + k_{22}C_\mathrm{sed2}) - \lambda C \\
\frac{\partial C_\mathrm{s}}{\partial t} &= (\mathrm{adv}+\mathrm{dif}) + \chi_{11}\frac{3}{\rho R}C - k_{21}C_\mathrm{s} - \lambda C_\mathrm{s} \\
\frac{\partial C_\mathrm{sed1}}{\partial t} &= \chi_{11}\frac{3\Psi}{\rho_\mathrm{b}R}C - k_{21}\Psi C_\mathrm{sed1} - \lambda C_\mathrm{sed1} \\
\frac{\partial C_\mathrm{sed2}}{\partial t} &= \chi_{12}\frac{3\Psi}{\rho_\mathrm{b}R}C - k_{22}\Psi C_\mathrm{sed2} - \lambda C_\mathrm{sed2}
\end{aligned} \tag{A9}$$

In these equations C and C_s are activity concentrations in the dissolved phase and suspended matter particles, respectively, and C_sed1 and C_sed2 are activity concentrations in the sediments (exchangeable and slowly reversible fractions, respectively), S_m is the concentration of suspended matter in water (kg m^{-3}). Also, indices 1,1 and 2,1 correspond to the fast reaction and indices 1,2 and 2,2 to the slower one. The last equations were used for the second phase of the exercise (application to 1999 flood). The values of parameters χ_{11}, χ_{12}, k_{21} and k_{22} are reported in Table A1.

A.2. ENEA

The river and the floodplain were subdivided, respectively, into 3 and 12 sectors. Each sector is identified by two indices: i (from 1 to 3) and j (from 1 to 5). The following equations were used to predict the total contents (Bq) of radionuclide in the water (T_wd = dissolved form and T_wp = particulate form) and in the soil or sediment active layer (T_s) of each sector i,j:

$$\begin{aligned}
\frac{\mathrm{d}T_\mathrm{wd}(i,j)}{\mathrm{d}t} &= -k_{12}T_\mathrm{wd}(i,j) + k_{21}T_\mathrm{wp}(i,j) - K_\mathrm{dws}T_\mathrm{wd}(i,j) - \lambda T_\mathrm{wd}(i,j) + I_\mathrm{d} - O_\mathrm{d} \\
\frac{\mathrm{d}T_\mathrm{wp}(i,j)}{\mathrm{d}t} &= +k_{12}T_\mathrm{wd}(i,j) - k_{21}T_\mathrm{wp}(i,j) - K_\mathrm{pws}T_\mathrm{wp}(i,j) + K_\mathrm{sw}T_\mathrm{s}(i,j) \\
&\quad - \lambda T_\mathrm{wp}(i,j) + I_\mathrm{p} - O_\mathrm{p} \\
\frac{\mathrm{d}T_\mathrm{s}(i,j)}{\mathrm{d}t} &= K_\mathrm{dws}T_\mathrm{wd}(i,j) + K_\mathrm{pws}T_\mathrm{wp}(i,j) - (K_\mathrm{sw}+K_\mathrm{ds})T_\mathrm{s}(i,j) - \lambda T_\mathrm{s}(i,j) \\
C(i,j) &= \frac{T_\mathrm{wd}(i,j)}{V(i,j)}
\end{aligned} \tag{A10}$$

$C(i,j)$ and $V(i,j)$ are the radionuclide concentration in water (dissolved form) and the volume of water in sector i,j. Compartment T_wp comprises the suspended matter in the water column and a thin surface layer of bottom sediment or soil (interface layer) that strongly interacts with

Table A1
Values of parameters in model "University of Sevilla-4C"

	^{90}Sr	^{137}Cs
χ_{11} (m s^{-1})	8.9×10^{-6}	1.4×10^{-5}
χ_{12} (m s^{-1})	8.9×10^{-7}	1.6×10^{-9}
k_{21} (s^{-1})	1.0×10^{-4}	1.2×10^{-5}
k_{22} (s^{-1})	1.8×10^{-5}	8.7×10^{-9}

radionuclide dissolved in water (Monte, 1995). I_d and I_p are the fluxes to the target sector i,j of dissolved and particulate radionuclide, respectively, from the contiguous sectors. Similarly, O_d and O_p are the fluxes from the target sector to the contiguous ones. k_{12} and k_{21} are, respectively, the rates of transformation of radionuclide from dissolved to particulate phase and vice versa. K_{dws} is the migration rate of dissolved radionuclide from water to sediment, K_{pws} is the migration rate of particulate radionuclide from the water column to sediment, K_{sw} is the migration rate of radionuclide from sediment to the water column. K_{ds} is the burial rate of radionuclide. The following hypotheses underlie the model:

(1) the concentrations of contaminant in compartments T_{wd} and T_{wp} reach a fast equilibrium

$$\frac{T_{wp}}{T_{wd}} = \frac{k_{12}}{k_{21}} = \frac{C_s(S_m hS + d\delta S)}{CSh} = k_d S_m + \frac{k_d d\delta}{h} = f_{p/d} + \frac{\Delta h}{h} \tag{A11}$$

where S_m is the concentration of suspended matter in water (kg m^{-3}), C_s is the concentration of radionuclide in particulate form (Bq kg^{-1}), h is the water column depth (m), S is the sector surface (m^2) and d and δ are, respectively, the thickness (m) and the density (kg m^{-3}) of the interface layer. $k_d = C_s/C$ is the partition coefficient (m^3 kg^{-1}), $f_{p/d} = k_d S_m$ is the fraction "radionuclide in particulate form (Bq m^{-3})/radionuclide in dissolved form (Bq m^{-3})" and $\Delta h = k_d d\delta$, whose dimension is a length, is the so-called "incremental depth" of the water body sector;

(2) the fluxes of contaminant from water to sediment are proportional to the concentration

$$\begin{aligned} \varphi_d &= v_{ds} C \\ \varphi_p &= v_{ps} C \end{aligned} \tag{A12}$$

where v_{ds} and v_{ps} are the velocity of deposition of dissolved and particulate radionuclide.

Therefore (S is the sector surface):

$$\begin{aligned} K_{dws} T_{wd}(i,j) &= \varphi_d S = S v_{ds} C = \frac{v_{ds}}{h} T_{wd}(i,j) \\ K_{pws} T_{wp}(i,j) &= \varphi_p S = S v_{ps} C = \frac{v_{ps}}{h} T_{wd}(i,j) \end{aligned} \tag{A13}$$

The total radionuclide flux from the water column to the bottom sediment is

$$\varphi_d S + \varphi_p S = \left(\frac{v_{ps}}{h} + \frac{v_{ds}}{h}\right) T_{wd}(i,j) = \frac{v_{ws}}{h} T_{wd}(i,j) \tag{A14}$$

where v_{ws} is the total velocity of deposition of radionuclide.

From hypothesis (1) we obtain that system (A10) can be approximated as follows:

$$\begin{aligned} \frac{dT_{wd}(i,j)}{dt} &= -k_{12} T_{wd}(i,j) + \frac{k_{12}}{f_{p/d} + \frac{\Delta h}{h}} T_{wp}(i,j) - \frac{v_{ws}}{h} T_{wd}(i,j) - \lambda T_{wd}(i,j) + I_d - O_d \\ \frac{dT_{wp}(i,j)}{dt} &= +k_{12} T_{wd}(i,j) - \frac{k_{12}}{f_{p/d} + \frac{\Delta h}{h}} T_{wp}(i,j) + K_{sw} T_s(i,j) - \lambda T_{wp}(i,j) + I_p - O_p \\ \frac{dT_s(i,j)}{dt} &= \frac{v_{ws}}{h} T_{wd}(i,j) - (K_{sw} + K_{ds}) T_s(i,j) - \lambda T_s(i,j) \\ C(i,j) &= \frac{T_{wd}(i,j)}{V(i,j)} \end{aligned} \tag{A15}$$

Indeed the fast equilibrium between compartments T_{wd} and T_{wp} implies that the total flux of radionuclide migrating from the water column to the bottom sediment can be attributed to compartment T_{wd} without a significant influence on the equation solutions. Dividing by the box surface the first and second members of Eq. (A15) we get:

$$\begin{aligned}
\frac{dhC(i,j)}{dt} &= -k_{12}hC(i,j) + \frac{k_{12}}{f_{p/d} + \frac{\Delta h}{h}} D_f(i,j) - \frac{v_{ws}}{h} hC(i,j) - \lambda hC(i,j) + I_d - O_d \\
\frac{dD_f(i,j)}{dt} &= +k_{12}hC(i,j) - \frac{k_{12}}{f_{p/d} + \frac{\Delta h}{h}} D_f(i,j) + K_{sw}D_s(i,j) - \lambda D_f(i,j) + I_p - O_p \\
\frac{dD_s(i,j)}{dt} &= \frac{v_{ws}}{h} hC(i,j) - (K_{sw} + K_{ds})D_s(i,j) - \lambda D_s(i,j)
\end{aligned} \tag{A16}$$

The concentration (C_{tot}) of total radionuclide in water is $C_{tot} = C(1 + f_{p/d})$.

The values of k_{12} and k_{21} are supposed $\to \infty$ (as required by hypothesis 1) while the ratio (A11) is constant. The fluxes I_d, I_p, O_d and O_p are calculated as the product of the water flowing between contiguous box multiplied by the radionuclide concentration in water plus a term simulating the turbulent diffusion of radionuclide in water. Such a term is supposed to be (a) directly proportional to the difference in radionuclide concentrations in the sectors; (b) directly proportional to the area of the interface between the sectors; and (c) inversely proportional to the distance between the centres of the sectors.

The hydraulic model is a crude approximation of the complex processes controlling the water fluxes. Nevertheless it can be considered appropriate for the aim of the present model whose uncertainty is mainly related to the processes of migration of radionuclide from the floodplain soil to water and vice versa. The fluxes of water between two contiguous sectors are supposed to be proportional to the differences in the water levels. Using this approximation the flooding of floodplain areas at different altitude levels was predicted. The water volume in the ''floodplain-river channel'' system was calculated from the balance of the inflowing water and the water outflow.

The model was solved using Powersim® version 2.5 software (Powersim Corporation, 12007 Sunrise Valley Drive, Reston, VA 22091, USA) running on a personal computer.

The values of the model parameters relevant to the processes of migration of radionuclide from the water column to the bottom sediments and vice versa are reported in Table 3.

The mathematical approach for modelling in a simple way such a process is described in the literature (Monte, 2001, 1995).

A.3. COASTOX (developed by IMMSP)

The two-dimensional lateral-longitudinal radionuclide transport model COASTOX consists of modules describing overland flow, sediment transport, erosion/deposition processes, radionuclide transport in solute and on suspended sediments by the overland flow and contamination of upper soil layer.

The model was tested within different studies of the radionuclide transport in the Chernobyl zone (Zheleznyak and Voitsekhovich, 1991; Zheleznyak et al., 1992, 1997; Zheleznyak, 1997) and is included into the Hydrological Dispersion Module of the EU decision support system RODOS (Zheleznyak et al., 2001).

A.3.1. Overland flow

Two-dimensional overland flow equations are obtained by vertically averaging the three-dimensional equations over flow depth. These equations consist of a continuity equation and two momentum equations:

$$\frac{\partial h}{\partial t}+\frac{\partial}{\partial x_i}(u_i h)=0 \tag{A17}$$

$$\frac{\partial}{\partial t}(u_i h)+\frac{\partial}{\partial x_i}\left(u_j u_i h\right)+gh\frac{\partial \xi}{\partial x_i}+g\frac{n^2}{h^{1/3}}u_i\sqrt{u_1^2+u_2^2}=0 \tag{A18}$$

where t is time (s); x_i is the spatial Cartesian coordinates (m); h is the flow depth (m); u_i is the flow velocity in the x_i-direction (m s^{-1}); $\xi(x,y,t)$ is the free surface elevation (m); g is the acceleration of the gravity (m s^{-2}); n is the Manning roughness coefficient (s m$^{-1/3}$). Eqs. (A17) and (A18) are similar to Eq. (A1) in the University of Sevilla model. They do not include the Coriolis term, as it is negligible for this application, and use the Manning's formula for the bed friction coefficient.

Change of the bed surface elevation, $\eta(x,y,t)$ (m), is described by

$$\rho_b(1-\Phi)\frac{\partial \eta}{\partial t}=q_s-q_b \tag{A19}$$

where Φ is the porosity of soil (dimensionless); ρ_b is the density of soil matrix (kg m^{-3}); q_s and q_b are the deposition and erosion rates (kg m^{-2} s^{-1}), respectively.

Mass conservation for sediment yields to

$$\frac{\partial}{\partial t}(hS_m)+\frac{\partial}{\partial x_i}(u_i h S_m)=\frac{\partial}{\partial x_i}\left(hD_i\frac{\partial S_m}{\partial x_i}\right)-q_s+q_b \tag{A20}$$

where S_m is the suspended sediment concentration (kg m^{-3}); D_i is the coefficient of horizontal dispersion (m^2 s^{-1}).

The erosion rate and deposition rate are defined by the following relationships:

- for non-cohesive sediments

$$q_s=\max\{0,w_0(S_m-S^*)\};\quad q_s=\max\{0,E_r w_0(S^*-S_m)\} \tag{A21}$$

- for cohesive sediments

$$q_s=\max\left\{0,w_0 S_m\left(1-\frac{\tau}{\tau_d}\right)\right\};\quad \text{for deposition (Krone, 1962)}$$

$$q_b=\max\left\{0,M\left(\frac{\tau}{\tau_e}-1\right)\right\}\qquad \text{for erosion (Partheniades, 1962, 1965, 1971)}$$

where S^* is the concentration at equilibrium sediment transport capacity (kg m^{-3}); w_0 is the settling velocity of suspended particles (m s^{-1}); E_r is the overland flow erodibility coefficient; τ_d and τ_e are, respectively, the critical shear stress for deposition and erosion; τ is the bed shear stress (N m^{-2}); M is experimentally derived constant.

The total load transport equation developed by Van Rijn (1984a,b) is used to compute the concentration at equilibrium transport capacity for non-cohesive sediments.

A.3.2. Radionuclide transport by overland flow

The radionuclide transport in the aqueous phase and on suspended sediments by overland flow is simulated by the following equations describing physical–chemical interactions and erosion–deposition exchange processes

$$\begin{aligned}
&\frac{\partial}{\partial t}(hC)+\frac{\partial}{\partial x_i}(u_i hC)=\frac{\partial}{\partial x_i}\left(hD_i\frac{\partial C}{\partial x_i}\right)-\lambda hC-a_s hS_m\left(\frac{k_d^s}{\rho}C-C_s\right)\\
&\qquad\qquad -(1-\Phi)La_b\left(k_d^b\frac{\rho_b}{\rho}C-C_b\right)\\
&\frac{\partial}{\partial t}(hS_mC_s)+\frac{\partial}{\partial x_i}(u_i hS_mC_s)=\frac{\partial}{\partial x_i}\left(hD_i\frac{\partial S_mC_s}{\partial x_i}\right)-\lambda hS_mC_s+a_s hS_m\left(\frac{k_d^s}{\rho}C-C_s\right)\\
&\qquad\qquad +\frac{1}{\rho_b}q_bC_b-q_sC_s\\
&\frac{\partial}{\partial t}\left(hS_mC_s^f\right)+\frac{\partial}{\partial x_i}\left(u_i hS_mC_s^f\right)=\frac{\partial}{\partial x_i}\left(hD_i\frac{\partial S_mC_s^f}{\partial x_i}\right)-\lambda hS_mC_s^f+\frac{1}{\rho_b}q_bC_b^f-q_sC_s^f\\
&\frac{\partial}{\partial t}\left(hS_mC_s^p\right)+\frac{\partial}{\partial x_i}\left(u_i hS_mC_s^p\right)=\frac{\partial}{\partial x_i}\left(hD_i\frac{\partial S_mC_s^p}{\partial x_i}\right)-\lambda hS_mC_s^p+\frac{1}{\rho_b}q_bC_b^p-q_sC_s^p
\end{aligned}\tag{A22}$$

where C is the volumetric radionuclide activity in the aqueous phase (Bq m^{-3}); C_s is the radionuclide activity in exchangeable phase on suspended sediment (Bq kg^{-1}); C_b is the volumetric radionuclide activity in the exchangeable phase in upper soil layer (Bq m^{-3}); L is the thickness of the active upper soil layer (m); λ is the radionuclide decay constant (s^{-1}); k_d^s and k_d^b are the partition coefficients for ''water-suspended sediment'' and ''water-upper soil layer'' systems, respectively; a_s and a_b are the exchange rates for ''water-suspended sediment'' and ''water-upper soil layer'' systems (s^{-1}); C_s^f and C_s^p are the radionuclide activity in fixed phase and fuel particles on suspended sediment (Bq kg^{-1}); C_b^f and C_b^p are the volumetric radionuclide activity in fixed phase and fuel particles per soil solid volume in upper soil layer (Bq m^{-3}).

A.3.3. Contamination of upper soil layer

Contamination of the active upper soil layer is described by the equations

$$\begin{aligned}
&\frac{\partial}{\partial t}(LC_b)=a_bL\left(k_b^d\frac{\rho_b}{\rho}C-C_b\right)-\lambda LC_b-\frac{1}{1-\Phi}\left\{\frac{1}{\rho_b}q_bC_b-q_sC_s\right\}\\
&\frac{\partial}{\partial t}\left(LC_b^f\right)=-\frac{1}{1-\Phi}\left\{\frac{1}{\rho_b}q_bC_b^f-q_sC_s^f\right\}\\
&\frac{\partial}{\partial t}(LC_b^p)=-L\left(\lambda+\alpha_p\right)C_b^p-\frac{1}{1-\Phi}\left\{\frac{1}{\rho_b}q_bC_b^p-q_sC_s^p\right\}
\end{aligned}\tag{A23}$$

where α_p is the first-order constant of radionuclide leaching from fuel particles (s^{-1}). The last equation describes the leaching of radionuclides from the fuel particles and erosion–deposition processes for the fuel particles.

Table A2
Parameters used in simulations of COASTOX model

Radionuclide	k_d^b	k_d^s	a_b (s^{-1})	a_s (s^{-1})
^{90}Sr	0.3		1.2×10^{-9}	
^{137}Cs	4500	15 000	5.8×10^{-7}	5.8×10^{-6}

The equations for the exchangeable phase are as follows:

$$\begin{aligned}
\frac{\partial}{\partial t}(hC) &= (\text{adv} + \text{diff}) - a_s S_m \frac{k_d^s}{\rho} hC - (1-\Phi)\frac{La_b}{h} k_d^b \frac{\rho_b}{\rho} hC + a_s D_f + a_b D_s - \lambda hC \\
\frac{\partial}{\partial t} D_f &= (\text{adv} + \text{diff}) + a_s S_m \frac{k_d^s}{\rho} hC - a_s D_f - \frac{q_s}{S_m h} D_f + \frac{q_b}{\rho_b (1-\Phi) L} D_s - \lambda D_f \\
\frac{\partial}{\partial t} D_s &= (1-\Phi)\frac{La_b}{h} k_d^b \frac{\rho_b}{\rho} hC + \frac{q_s}{S_m h} D_f - a_b D_s - \frac{q_b}{\rho_b (1-\Phi) L} D_s - \lambda D_s
\end{aligned} \tag{A24}$$

Table A2 shows a selection of values of parameters used by COASTOX model.

References

BIOMASS, 2003. Testing of Environmental Transfer Models Using Chernobyl Fallout Data from the Iput River Catchment Area, Bryansk Region, Russian Federation. IAEA, Vienna, Austria, ISBN 92-0-104003-2.

BIOMOVS, 1990. On the validity of environmental transfer models. Proceedings of a Symposium, Stockholm, Sweden. Swedish Radiation Protection Institute, ISBN 91-630-0437-2. Printed by Sundt Artprint, Stockholm, Sweden.

BIOMOVS II, 1996. Assessment of the consequences of the radioactive contamination of aquatic media and biota. Technical Report No. 10. Swedish Radiation Protection Institute, Stockholm, Sweden. ISSN: 1103-055.

Frissel, M.J., Pennders, R., 1983. Models for the accumulation of ^{90}Sr, ^{137}Cs, $^{239,240}Pu$ and ^{241}Am in the upper layers of soil. In: Coughtrey, P.J. (Ed.), Ecological Aspects of Radionuclide Release. Blackwell, Oxford, U.K., pp. 63−72.

Håkanson, L., Monte, L., 2003. Radioactivity in lakes and rivers. In: Marian Scott, E. (Ed.), Modelling Radioactivity in the Environment. Elsevier Science Ltd., pp. 147−200.

IAEA, 2000. Modelling of the transfer of radiocaesium from deposition to lake ecosystems. Report of the VAMP Aquatic Working Group. IAEA-TECDOC-1143, Vienna, Austria.

Jørgensen, S.E., 1983. The modelling procedure. In: Jørgensen, S.E. (Ed.), Application of Ecological Modelling in Environmental Management, Part A. Elsevier Scientific Publishing Company, Amsterdam, The Netherlands, pp. 5−15.

Jørgensen, S.E., Mejer, H., 1979. A holistic approach to ecological modelling. Ecological Modelling 7, 169−189.

Krone, R.B., 1962. Flume studies of the transport of sediment in estuarial shoaling processes. Hydraulic Engineering Laboratory and Sanitary Engineering Research Laboratory, University of California at Berkeley, California.

Livens, F.R., Rimmer, D.L., 1988. Physico-chemical controls on artificial radionuclides in soil. Soil Use and Management 4, 63−69.

McHenry, J.R., Ritchie, J.C., 1977. Physical and chemical parameters affecting transport of 137Cs in arid watershed. Water Resources Research 13, 923−927.

Monte, L., 1995. A simple formula to predict approximate initial contamination of lake water following a pulse deposition of radionuclide. Health Physics 68, 397−400.

Monte, L., 2001. A generic model for assessing the effects of countermeasures to reduce the radionuclide contamination levels in abiotic components of fresh water systems and complex catchments. Environmental Modelling & Software 16, 669−690.

Monte, L., Brittain, J.E., Håkanson, L., Heling, R., Smith, J.T., Zheleznyak, M., 2003. Review and assessment of models used to predict the fate of radionuclides in lakes. Journal of Environmental Radioactivity 69, 177−205.

Monte, L., Brittain, J.E., Håkanson, L., Smith, T.J., van der Perk, M., 2004. Review and assessment of models for predicting the migration of radionuclides from catchments. Journal of Environmental Radioactivity 75, 83−103.

Monte, L., Boyer, P., Brittain, J.E., Håkanson, L., Lepicard, S., Smith, J.T., 2005a. Review and assessment of models for predicting the migration of radionuclides through rivers. Journal of Environmental Radioactivity 79, 273−296.

Monte, L., Hofman, D., Brittain, J. (Eds.), 2005b. Evaluation and network of EC-decision support systems in the field of hydrological dispersion models and of aquatic radioecological research. Technical report. RT/2005/49/PROT, ENEA, Rome, Italy.

Partheniades, E., 1962. A study of erosion and deposition of cohesive soils in salt water. Thesis presented to the University of California at Berkeley, California.

Partheniades, E., 1965. Erosion and deposition of cohesive soils. Journal of the Hydraulics Division, ASCE 91, 105−139.

Partheniades, E., 1971. Unified view of wash load and bed material load. Journal of the Hydraulics Division, ASCE 103, 1037−1057.

Periáñez, R., 2004. Testing the behaviour of different kinetic models for uptake-release of radionuclides between water and sediments when implemented on a marine dispersion model. Journal of Environmental Radioactivity 71, 243−259.

Ritchie, J.C., McHenry, J.R., 1990. Application of radioactive fallout 137Cs for measuring soil erosion and sediment accumulation rates and patterns: a review. Journal of Environmental Quality 19, 215−233.

Smith, J.T., Voitsekhovitch, O.V., Håkanson, L., Hilton, J., 2001. A critical review of measures to reduce radioactive doses from drinking water and consumption of freshwater foodstuffs. Journal of Environmental Radioactivity 56, 11−32.

Van Rijn, L.C., 1984a. Sediment transport, part I: bed load transport. Journal of Hydraulic Engineering, ASCE 110, 1431−1456.

Van Rijn, L.C., 1984b. Sediment transport, part II: suspended load transport. Journal of Hydraulic Engineering, ASCE 110, 1613−1641.

Voitsekhovich, O.V., Borzilov, V.A., Konoplev, A.V., 1991. Hydrological aspects of radionuclide migration in water bodies following the Chernobyl accident. In: Proceedings of Seminar on Comparative Assessment of the Environmental Impact of Radionuclides Released during Three Major Nuclear Accidents: Kyshtym, Windscale, Chernobyl, Luxembourg, 1−5 October 1990, vol. 1. Commission of the European Communities, Radiation Protection-53, EUR 13574, pp. 527−548.

Voitsekhovich, O.V., Laptev, G., Konoplev, A.V., Bulgakov, A., 2004. The floodplain scenario. <http://www-ns.iaea.org/projects/emras/>.

Zheleznyak, M., Voitsekhovich O.V., 1991. Mathematical modelling of radionuclide dispersion in surface waters after the Chernobyl accident to evaluate the effectiveness of water protection measures. In: Proceedings of Seminar on Comparative Assessment of the Environmental Impact of Radionuclides Released during Three Major Nuclear Accidents: Kyshtym, Windscale, Chernobyl, Luxembourg, 1−5 October 1990, vol. 2. Commission of the European Communities, Radiation Protection-53, EUR 13574, pp. 725−748.

Zheleznyak, M., Demchenko, R.I., Khursin, S.L., Kuzmenko, Y.I., Tkalich, P.V., Vitiuk, N.Y., 1992. Mathematical modeling of radionuclide dispersion in the Pripyat-Dnieper aquatic system after the Chernobyl accident. The Science of the Total Environment 112, 89−114.

Zheleznyak, M., 1997. Multiple scale analyses of radioactive contamination for rivers and reservoirs after the Chernobyl accident. Multiple Scale Analyses and Coupled Physical Systems. Proceedings of Saint-Venant Symposium, August 28−29, 1997. Presses de l'ecole nationale des ponts et chaussees, Paris, pp. 45−52.

Zheleznyak, M., Shepeleva, T., Sizonenko, V., Mezhueva, I., 1997. Simulation of countermeasures to diminish radionuclide fluxes from Chernobyl zone via aquatic pathways. Radiation Protection Dosimetry 73, 181−186.

Zheleznyak M., Heling R., Raskob W., 2001. Hydrological dispersion module of the decision support system RODOS. In: Proceedings of Conference ECORAD-2001, Aix-en-Provance, France, 3−6 September, 2001.